

BRENO TOTTI MAIA^{1,2}, WILLIAN DOS REIS LIMA^{1, 2}, ROMÁRIO DA ROCHA NASCIMENTO², FELIPE DA SILVEIRA BATISTA¹, DANIEL AUGUSTO GODINHO DE CARVALHO³, CAIO NOGUEIRA ARAÚJO DINIZ⁴, DANIELA LADEIRA DE SOUZA⁴, RAISSA SANTOS SALGADO⁴, ROBERTO PARREIRAS TAVARES⁴

APPLICATION OF THE SIMILARITY METHOD FOR COLD MODELING A 330 TONS BOF CONVERTER IN LABORATORY

Abstract

Noticed the strong national and international industrial activity, more specifically concerning the steel production and the model of oxygen converter adopted on the different types of primary refining process, this work applies to relevant models, reevaluating since the more rudimentary techniques till the current technologies. Then they will present the methods in which resulted the study of similarity in a converter 330 tons bringing to a 1/10 scale, allowing the realization of the studies in laboratory. Right after, will be performed an analysis comparison between simulation cold versus hot showing the benefits and drawbacks in working with the two situations. Ultimately, intends to show the deferens costs in carrying out a simulation to cold and hot simulation and also present the benefits to perform simulation in the cold model. The results obtained after the stage of discussion were satisfactory, since it allowed to reach plausible conclusions which will be of great value to companies that have the need for process improvement at low cost and without taking big risks.

Keywords:

BOF; Modeling; Cold tests; Similarity.

¹ Lumar Metals Ltda. Highway MG 232, km 09, N° 100, Santana do Paraíso, MG, Brazil, ZIP Code: 35.179-000

² University Center of the East of Minas Gerais –Unileste, - Av.Tancredo Neves, 3500, University District, MG,Brazil, ZIP Code: 35170-056056

³ CSA Thyssen Krupp Avenue João XXIII Santa Cruz, Rio de Janeiro, Brazil ZIP Code: 23560-352

⁴ Federal University of Minas Gerais (UFMG) Avenue Antônio Carlos, 6627, Pampulha Belo Horizonte, Minas Gerais, Brazil ZIP Code: 31270-901

1. Introduction

The market requirements in search of an efficient product, low cost and competitive in addition to the need to comply at legislations in environmental and safety issues, has made the big steelmakers use laboratory methods to develop their products and improve their processes.

Thinking about this, Thyssen Krupp CSA, with a partnership between the company Lumar Metals and the Federal University of Minas Gerais (UFMG), started a project in which the objective was to improve metallurgical processes, the configuration of tuyeres (TBM process) and too oxygen lance through cold molding performed on laboratory scale.

The method used was realized through method cold molding and geometrical similarity and metallurgic process, which aims to seek the real data in industry and retransmit for laboratory allowing your simulation. The cold model has the objective to seek approximate to the maximum the industrial process, under much lower temperatures.

2. Methods and Materials

In cold modeling in LD converter, the refractory usually is substituted for acrylic structure and utilized water with objective simulate the metal bath. Normally, water it is the fluid used to represent liquid steel, due your properties as cinematics viscosities are similar. The table 1 below to show the comparison between properties the steel and water.

PROPERTIES	UNIT	SYMBOL	WATER	STEEL
Temperature	°C	T	25	1600
Dynamic Viscosities	kg.m ⁻¹ .s ⁻¹	μ	1,0x10 ⁻³	6,4x10 ⁻³
Cinematics Viscosities	m ² .s ⁻¹	ν	1,00x10 ⁻⁶	9,13x10 ⁻⁷
Density	kg.m ⁻³	ρ	1,00x10 ³	7,08x10 ³
Superficial Tension	N.m ⁻¹	σ	0,0728	1,6

Table 1 Comparison between proprieties of the water and steel ^[1]

It is necessary that the solutions related to the model and the industrial machine are similar, before this it is necessary that there be similarity, starting with the geometry and then the metallurgical parameters through similarities cinematics and dynamic.

This way, to obtain and equalize this information for the continuity of the study was inserted the process of similarity.

2.1. Geometrical similarity and process metallurgical

For this study the dimension used for scale factor was the diameter of the converter, which is presented in Figure 1 and represented by equation 1 below.

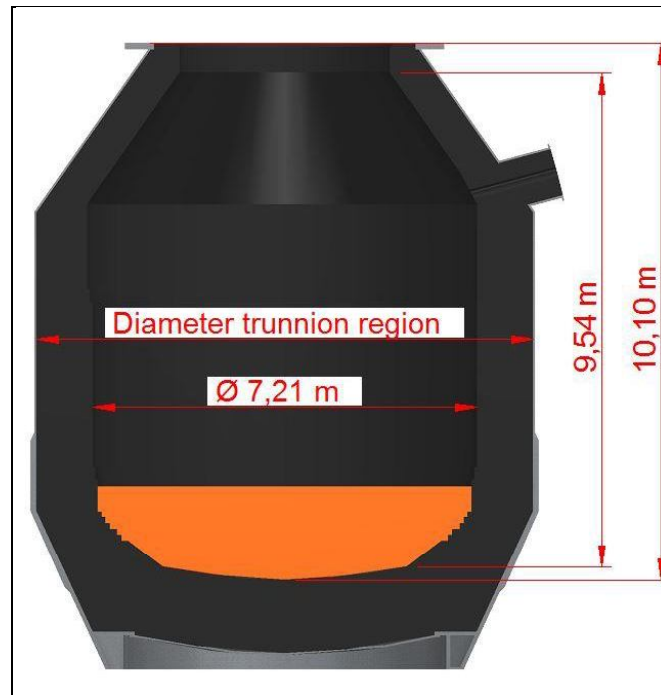


Figure 1 BOF industrial scale [2]

$$\lambda = \frac{D_{BOF}^{CM}}{D_{BOF}^{IND}} = \frac{1}{10} \quad (\text{Equation 1})$$

Where: “ λ ” – scale factor, “ D_{BOF}^{CM} ” – diameter trunnion region of the BOF cold model (m), “ D_{BOF}^{IND} ” – diameter trunnion region of the BOF industrial (m).

Next, Table 2 presents the main dimensions of the industrial model (real scale) as well as the dimensions of what should be the cold model for laboratory simulation.

ABBREVIATIONS	UNIT	DATA ENTRY	INDUSTRIAL MODEL 330 T (HOT)	LABORATORY MODEL330T (COLD)
		Scale	1	1/10
D_{conv}	m	Furnace diameter	7,156	0,716
H^{real}	m	Furnace height	10,086	1,009
H_b	m	Metal bath height	1,715	0,1715
H	m	Distance bath lance	2,200	0,451
-	-	Diameter scale	1	1/10
-	-	Height scale	1	1/10
-	-	Level scale	1	1/10
$D_{SAÍDA}$	m	Outlet Diameter	0,0606	0,0033
D^*	m	Throat Diameter	0,0439	0,0026
D_o	m	Diameter for Stagnant Condition	0,0621	0,0037
H_{FURO}	m	Hole to Output Height	0,0860	0,0150
	degrees	Divergent Cone Angle	11°	2,5°
$L_{SAÍDA}$	m	Distance Center TIP-Center hole	0,087	0,0041
NF	#	Number of holes TIP	6	6

Table 2 Main dimensions and scale relationships [1]

After the scale was defined for the reduction of the converter and the geometric similarity was realized, the design of the acrylic converter model was realized.

To achieve a feasible project, easy execution and low cost, small adjustments were made to the internal profile of the converter, removing the steps leaving the project in the lowest degree of details possible.

How much more detail, the greater the need for skilled labor, specific tooling and longer execution time, this way the costs of manufacturing increase. It is important to note that the simplification changes were made to keep the original characteristics of the converter as much as possible and to keep the volume of the static bath level as close as possible. In this way, the results obtained can be verified in Figure 2 below.

It is important to verify that for the realization of the design of the acrylic converter, only the internal profile of the converter was considered, because it is occupied by the liquid metal and the transport phenomena occur in this volume during the refining operation of the pig iron in the steel.

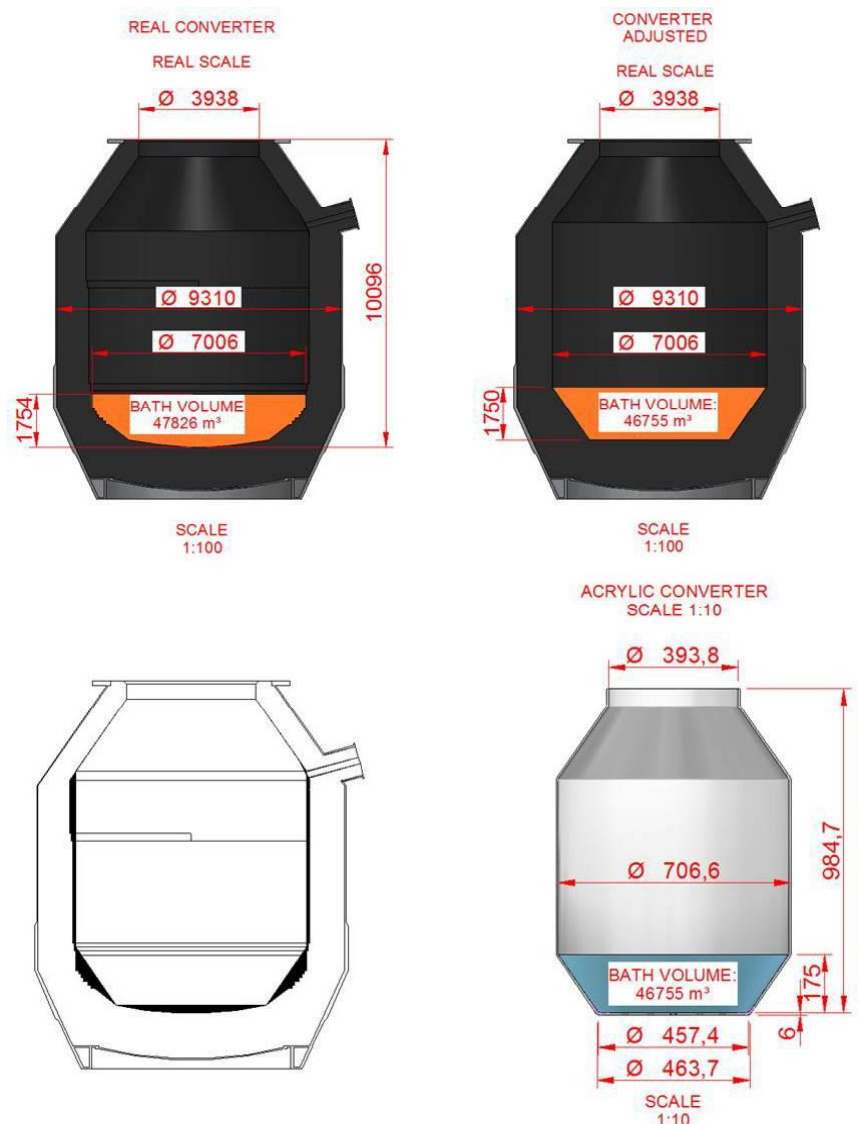


Figure 2 Adjusted converter^[2]

Finished this process, after realized all necessary adjusts, was realized the manufacture the acrylic converter and after of manufacture was installed at the dependences of Simulations process laboratory (LASIP), situated in Federal University of Minas Gerais (UFMG).

For sequence, was realizes the similarity of tip lance, objectifying to adapt to acrylic converter. The results, can be verified in table 3 below.

ABBREVIATIONS	UNIT	DATA ENTRY	INDUSTRIAL MODEL 330 T (HOT)	LABORATORY MODEL330T (COLD)
D_{SAIDA}	m	Exit diameter	0,0606	0,0033
D^*	m	Throat diameter	0,0439	0,0026
H_{FURO}	m	Hole to Output Height	0,086	0,015
\angle	degrees	Divergent Cone Angle	11°	2,5°

Table 3 TIP similarity ^[1]

For simulate the blow conditions, was utilized the compression equipment of air (compressor) the university, your nominal installation capacity corresponds the 180 Nm³/h, but reaching 160 Nm³/h (maximum) during the tests, thus objectifying similarity with the dimensionless Mach number, that can be verified in equation 2 below.

$$Ma = \frac{\bar{v}}{v_s} \quad (\text{Equation 2})$$

Where: “Ma” dimensionless Mach number, “v” average velocity (m.s⁻¹), “v_s” Sound velocity in the middle (m.s⁻¹).

Maia and Martins (2012), present the dimensionless number of Mach as a relation between the velocity of the fluid and the sound velocity in the middle. The figure 3 shows the image of a nozzle and within it the evolution of subsonic velocity to supersonic in relation to the area.

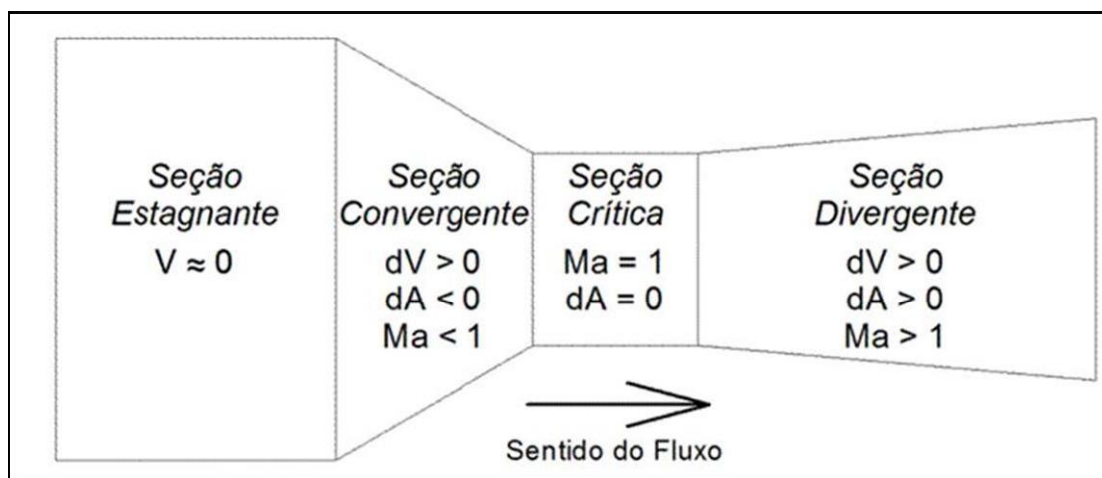


Figure 3 Entry and exit of a supersonic nozzle ^[3]

Due to the difference in pressure between the industrial reality and the cold model conditions and their impact on the Mach number, a geometric similarity scale was performed

distorted between the dimensions of the converter and the nozzle tip. Table 4 below shows the property of the jets comparing hot model and cold model.

To ensure equal dynamic similarities; relations between forces of the same nature; The boom height was used as the adjustment parameter. The adjustment consisted of maintaining the equality of the modified Froude dimensionless number developed in LASIP and presented by equation 3 below.

ABBREVIATIONS	UNIT	DATA ENTRY	INDUSTRIAL MODEL 330 T (HOT)	LABORATORY MODEL330T (COLD)
$P_{SAÍDA}/P_O$	#	Dimensionless pressure	0,07	0,15
$T_{SAÍDA}/T_O$	#	Dimensionless temperature	0,47	0,59
P^*	Pa	Pressure in critical section	833000,00	443000,00
r^*	kg/m ³	Density in critical section	12,86	6,19
T^*	K	Temperature in critical section	249,37	249,37
Ma	#	Mach Number	2,39	1,91
A/A* BOF p.134	#	Dimensionless area	2,41	1,57
A/A* Kawakami (1966)	#	Dimensionless area	2,51	1,75
A/A* Brahma Deo (2006)	#	Dimensionless area	1,91	1,22
$D_{SAÍDA}$	m	Nozzle exit diameter	0,06	0,00
$P_{SAÍDA}$	Pa	Nozzle exit pressure	108300,00	123800,00
$r_{SAÍDA}$	kg/m ³	Density at nozzle exit	2,96	2,47
$T_{SAÍDA}$	K	Temperature at nozzle exit	141,00	174,00
v_{SOM}	m/s	Sound velocity in the middle	225,00	264,00
$v_{SAÍDA}$	m/s	Nozzle exit velocity	540,00	503,00
$A_{SAÍDA}$	m ²	Nozzle exit area	0,00	0,00
$A_{TOTAL SAÍDA}$	m ²	Nozzles total exit area	0,02	0,00
$Q_{SAÍDA}$	m ³ /seg	Flow	9,34	0,03
$Q_{TOTAL SAÍDA}$	Nm ³ /min	Normalized flow	1187,38	2,66
	Nm ³ /h	Normalized flow	71243,00	159,70

Table 4 Jet properties

$$Fr^* = \frac{\rho_{gas} \times v_{EXIT}^2 \times D_{EXIT}^2 \times \cos \theta \times n}{\rho_{STEEL} \times g \times DBL^3} \quad (\text{Equation 3})$$

Where: “Fr*” – modified Froude dimensionless number LASIP, relation between forces of inertia and gravitational forces, “g” – acceleration of gravity (m.s⁻²), “ρ_{steel}” – bath density (kg.m⁻³), “ρ_{gás}” – Density of the gas at the nozzle exit (kg.m⁻³), “V_{EXIT}” – velocity at the nozzle exit (m/s), “D_{EXIT}” – nozzle exit diameter (m/s), “θ” – exit angle with vertical, “n” – number of nozzles.

In order to simplify calculations bath was considered monophasic, that is, only metallic bath, as shown in table 5 below.

ABBREVIATIONS	UNIT	DATA ENTRY	INDUSTRIAL MODEL 330 T (HOT)	LABORATORY MODEL330T (COLD)
	mm	Distance bath lance (DBL)	2200	451
D_{SAIDA}	m	Exit diameter	0,0606	0,0033
D^*	m	Diameter throat	0,0439	0,0026
D_o	m	Diameter for Stagnant Condition Bath	0,0621 Liquid steel	0,0037 Water
ρ	kg/m ³	Density	6930	1000
μ	kg/m.s = Pa.s	Dynamic Viscosity Steel	0,0055	0,001
V_{SAIDA}	m/s	Nozzle exit velocity	540	503
q	graus	Inclination of the Injector	17,5	17,5
Fr^*	#	Froude Modified monophasic LASIP	0,135	0,135

Table 5 Dimensional Comparison of Froude.

Determined the geometric and dynamic similarity considering only blow by the top, it remains to define cold simulation parameters considering two other important process factors: slag layer and submerged blow.

The slag has an important aspect in the penetration and movement of the bath, because it has high surface tension and low density when compared with the liquid bath. In this sense the dimensionless that contemplates these parameters is the number of Weber, which is presented in equation 4 below.

$$We = \frac{\rho_{gas} \times V_{EXIT}^2}{\rho_{STEEL} \times g \times \sigma_{STEEL}} \quad (\text{Equation 4})$$

Where: “We” – dimensionless number of Weber, relation between forces of inertia and forces of surface tension, “g” – acceleration of gravity (m.s⁻²), “ ρ_{gas} ” – density of the gas at the nozzle exit (kg.m⁻³), “ ρ_{steel} ” – bath density (kg.m⁻³), “ σ_{steel} ” – metal surface tension (N.m⁻¹), “ V_{exit} ” – velocity at the nozzle exit (m/s).

The Weber number is the ratio between the inertial force of the oxygen jet (causing the cavity, the ejection of metal droplets) and the forces of the metal mass and interfacial tension (responsible for the integrity of the bath), also slag, but in this equation presented only one phase. For the experiments, we developed the Weber Biphasic Modified Weber LASIP equation presented in equations 5 and 6 below and represented in Table 6:

$$We^{BI} = \frac{\rho_{gas} \times V_{EXIT}^2 \times D_{EXIT}^2}{(H_{BL} + H_{SL}) \times (\sigma_{STEEL} + \sigma_{SLAG})} \quad (\text{Equation 5})$$

$$We^{*LASIP} = \frac{P^2 \times (\rho_{STEEL} + \rho_{SLAG}) \times g}{\cos \theta \times (\sigma_{STEEL} + \sigma_{SLAG})} \quad (\text{Equation 6})$$

Where: “ We^{*BI} ” – dimensionless number of Weber two-phase metal system, slag, “ We^{*LASIP} ” – dimensionless number of Weber two-phase metal system, slag, “ ρ_{gas} ” – density

of the gas at the nozzle exit ($\text{kg}\cdot\text{m}^{-3}$), “ V_{EXIT} ” – velocity at the nozzle exit (m/s), “ D_{EXIT} ” – nozzle exit diameter (m), “ H_{BL} ” – static metal bath height (m), “ H_{SL} ” – static slag height (m), “ σ_{STEEL} ” – metal surface tension ($\text{N}\cdot\text{m}^{-1}$), “ σ_{SLAG} ” – surface tension of slag ($\text{N}\cdot\text{m}^{-1}$), “ g ” – acceleration of gravity ($\text{m}\cdot\text{s}^{-2}$), “ ρ_{steel} ” – bath density ($\text{kg}\cdot\text{m}^{-3}$), “ ρ_{SLAG} ” – density of slag ($\text{kg}\cdot\text{m}^{-3}$), “ P ” – penetration (m).

ABBREVIATIONS	UNIT	DATA ENTRY	INDUSTRIAL MODEL 330 T (HOT)	LABORATORY MODEL330T (COLD)
$We_{*\text{MONO}}$	#	Weber modified monophasic	8,59E+03	8,24E+02
$We_{*\text{BI}}$	#	Weber modified Biphasic	6,97E+03	1,14E+03
$We_{*\text{LASIP}}$	#	Weber modified LASIP	5,042E+04	2,534E+03

Table 6 Dimensionless comparison Weber

Another factor to be considered is that the individual jets incorporate surrounding mass as they travel from the boom spout to the bath surface. The opening of their cones can be such that they lead to interaction and coalescence between them. Furthermore, they can be decelerated by friction against the surrounding environment. In this way, the greater the distance of the bath, the smaller the force due to the inertia of the jet acting on the liquid; Which can be quantified as a function of a Moment number, in Equation 7 below, already with subscripts adjusted for condition of the proposed hour.

$$M = \frac{\rho_{\text{gas}} \times V_{\text{EXIT}}^2 \times D_{\text{EXIT}}^2}{\rho_{\text{MIXER}} \times g \times \text{DBL}^3} \quad (\text{Equation 7})$$

Where: “ M ” – Dimensionless moment number, relation between forces kinetics and gravitational forces, “ ρ_{gas} ” – density of the gas at the nozzle exit ($\text{kg}\cdot\text{m}^{-3}$), “ V_{EXIT} ” – velocity at the nozzle exit (m/s), “ D_{EXIT} ” – nozzle exit diameter (m), “ ρ_{MIXER} ” – density of the average of the bath considering metal, slag and injected gas ($\text{kg}\cdot\text{m}^{-3}$), “ g ” – acceleration of gravity ($\text{m}\cdot\text{s}^{-2}$), “ DBL ” – distance bath lance (m).

In equation 7 above the density of the mixture is represents to, “ ρ_{mixer} ”, which represents the average density of the metal bath, slag and inert gas mixture is presented. The density of the blend has a lower density than the metal bath and as an effect promotes elevation of the level occupied, with direct impact on jet penetration. This parameter is a direct response of the flow of inert gas injected by the bottom. Comparing the level of the static bath, with the increase of the bubbling flow the density of the bath gradually decreases and the level of bath rising. For effects of calculation of similarity was considered at the same instant of time, the injected gas is homogeneously distributed in the bath, in other words, considering the liquid bath as a system, there is only the mass input for a given moment of time, but of form not cumulative. The dimensionless Moment was used to adjust the total flow of the submerged blow of the experiment in relation to the industrial reality. This dimensionless was calculated using two calculation sequence criterion. The first criterion considers only the value of NG that will be further explained and has the moment balance only as a calculation response. The second criterion uses the dimensionless Moment as reference to reach the value close to the industrial one as shown in table 7.

ABBREVIATIONS	UNIT	DATA ENTRY	INDUSTRIAL MODEL 330 T (HOT)	LABORATORY MODEL330T (COLD)
	#	Distance bath lance (DBL)	2700	554
	Nm ³ /h	Tuyeres flow	70,00	0,912
	#	Moment	0,00351	0,01458

Tabela 7 Comparação adimensional de Momento

A brief explanation on the first criterion using the dimensionless "NG" denominated dimensionless of Mass Speed according to equation 8 below:

$$N_G = \frac{\rho_{IG} \times V_{IG}}{\rho^* \times V^*} \quad (\text{Equação 8})$$

Where: "NG" – Dimensionless of Mass, "ρ_{IG}" – Density of the inert gas at the working temperature and pressure (kg.m⁻³), "V_{IG}" – Velocity of inert gas in tuyeres (m/s), "ρ*" – Density of the inert gas (1bar, 20°C) (kg.m⁻³), "V*" – Speed of sound in the air (1bar, 20°C) (m/s).

For the experiment, the values shown in Table 7

ABBREVIATIONS	UNIT	DATA ENTRY	INDUSTRIAL MODEL 330 T (HOT)	LABORATORY MODEL330T (COLD)
#	Nm ³ /h	Flow	720	9,38
#	Nm ³ /h	Flow	840	10,94
#	Nm ³ /h	Flow	12	0,156296
#	Nm ³ /h	Flow	14	0,182345
#	#	NG	0,8	0,785772

Table 8 Dimensional comparison of Mass velocity.

In the second proposal, in the value of "ρ_{MIXER}", again influenced mainly by the inert gas flow, this was calculated using as a similarity factor a direct ratio of the top blow-off between industry and cold model, dividing the inert gas injection value of the industry, as shown in table 9.

By comparing the "mixer" results presented as the average density of the bath, it is possible that the density ratio of the mixture to density of the metal bath in none of the cases gives the reference value calculated for industrial mainly due to the difference in density of the liquid metal, but in the meantime, considering the adjustment of the bubbling flow by the dimensionless moment the relation was close.

High number of Reynolds indicates turbulent regime. In this case Reynolds reflects only the condition of the metal bath and the main reason for difference of values between the industrial practice and the model is the large difference in density between the metal and water and the speed limitation in the model due to the working pressure of the compressor. The Table 10 below presents the comparison between the dimensionless Reynolds between hot model and cold model.

ABBREVIATIONS	UNIT	DATA ENTRY	INDUSTRIAL MODEL 330 T (HOT)	LABORATORY MODEL330T (COLD)
#	Nm ³ /min./total	flow	12	0,156
#	Nm ³ /h/total	flow	720	1,614
#	kg/min./total	Mass flow	19,19	0,03
#	kg/m ³	Average Density of Bath	4,80	718,97
#	m ³	Bath volume	80,926	0,108
#	%	% Increase volume	69,94	68,36
#	mm	Ventaneira level	828,13	108,78
#	#	Density Mixture / Metallic Bath	69,28	71,90

Table 9 Comparison of the properties of the phases of the industry and cold model.

Finishing this step to characterize the turbulent regime in both conditions were used the Reynolds number modified according to equation 9 below:

$$Re^* = \left(\frac{V_{EXIT}^2 \times D_{EXIT}^2 \times \rho_{gas} \times \rho_{STEEL}}{\nu_{STEEL}^2} \right)^{\frac{1}{2}} \quad (\text{Equation 9})$$

Where : “Re*” – dimensionless number of Reynolds, relation between inertial forces and viscous forces, “ ρ_{gas} ” – density of the gas at the nozzle exit (kg.m⁻³), “V_{exit}” – velocity at the nozzle exit (m/s), “D_{exit}” – Nozzle exit diameter (m), “ ρ_{steel} ” – bath density (kg.m⁻³), “ ν_{steel} ” – dynamic viscosity of the metal bath (m²/s).

ABBREVIATIONS	UNIT	DATA ENTRY	INDUSTRIAL MODEL 330 T (HOT)	LABORATORY MODEL330T (COLD)
Re*	#	Modified Reynolds	8,523E+05	8,279E+04

Table 10 Dimensionless comparison Reynolds

4. Conclusions

With the accomplishment of this work it is possible to conclude:

1. Due to the large process variables, the risks (both for human life and environmental) in carrying out hot tests are high, while in laboratory tests the environment is safe and harmless to the environment;
2. In cold tests it is possible to extrapolate experiments, due to the low cost of execution and safety with people's lives;
3. Gains as operational stability can be obtained through cold tests.

5. Acknowledgments

The authors are grateful to Lumar Metals for the encouragement of research and development, the UFMG in special to Professor Roberto Parreiras, thyssenkrupp CSA for partnership, and to the University Center of the East of Minas Gerais (Unileste - MG), especially the brilliant team of teachers through shared teaching that enabled us to develop notorious works.

6. References

- [1] LUMAR METALS. Modelamento a frio convertedor BOF 330t. Belo Horizonte: LUMAR, 2016, p.13-22,
- [2] NASCIMENTO, Romário da Rocha; LIMA, Willian dos Reis. Configurações dos convertedores a oxigênio e parâmetros de operação. 2016.107 f. Trabalho de Conclusão de Curso (Engenharia Mecânica) - Centro Universitário do Leste de Minas Gerais (Unileste MG), Coronel Fabriciano, 2016. 2011, p.125-167.
- [3] MAIA, Breno Totti; MARTINS, Antônio Augusto. Lança de Oxigênio. In: ASSOCIAÇÃO BRASILEIRA DE METALURGIA, MATERIAIS E MINERAÇÃO. Aciaria a oxigênio. Rio de Janeiro: ABM, 2014.
- [4] MAIA, B. T., PETRUCELLI, A. C., DINIZ, C. N. A., SILVEIRA, D., ANDRADE, P. H. M. S., IMAGAWA, R. K., TAVARES, R. P., Comparação da Penetração do sopro de Oxigênio em Converteedores BOF com Bicos Multifuros utilizando Modelagem Física. Seminário de Aciaria Internacional. Porto Alegre, Maio 2014.
- [5] MAIA, Breno Totti. Efeito da configuração do bico da lança na interação jato-banho metálico em convertedor LD. 2007. 155 f. Dissertação (Mestrado em Engenharia Metalúrgica e de Minas) - Universidade Federal de Minas Gerais, Belo Horizonte, 2007.
- [6] MAIA, Breno Totti; IMAGAWA, Rafael Kajimoto; TAVARES, Roberto Parreiras. Cold model bath behavior study in BOF converter with bottom blowing. In: SEMINÁRIO DE ACIARIA - INTERNACIONAL ABM WEEK, 46., 2015, Rio de Janeiro, 2015. Anais... Rio de Janeiro: ABM, 2015.